ORIGINAL ARTICLE

Structural development of wheat nutrient transfer tissues and their relationships with filial tissues development

Yu Xurun · Chen Xinyu · Zhou Liang · Zhang Jing · Yu Heng · Shao Shanshan · Xiong Fei · Wang Zhong

Abstract Nutrients from spikelet phloem are commonly delivered to endosperm via caryopsis nutrient transfer tissues (NTTs). Elucidation of NTTs development is paramount to developing an understanding of the control of assimilate partitioning. Little information was available on the structural development of the entire NTTs and their functions, particularly those involved in the relationship between development of NTTs and growth of filial tissues including endosperm and embryo. In this study, wheat caryopses at different development stages were collected for observation of the NTTs by light microscopy, stereoscopic microscopy, and scanning electron microscopy. The cytological features of NTTs in the developing wheat caryopsis were clearly elucidated. The results were as follows: NTTs in the wheat caryopsis include maternal transfer tissues that are composed of vascular bundle, chalaza and nucellar projection transfer cells, and endosperm transfer tissues that consist of the aleurone transfer cells, starchy endosperm transfer cells, and endosperm conducting cells. The initiation, development, and apoptosis of these NTTs revealed the pattern of temporal and spatial gradient and were closely coordinated with endosperm and embryo development. These results may give us a further understanding about the functions of NTTs and their relationships with endosperm and embryo development.

Keywords Development · Endosperm transfer tissues · Maternal transfer tissues · Transfer cells · Wheat

Handling Editor: Jaideep Mathur

Y. Xurun · C. Xinyu · Z. Liang · Z. Jing · Y. Heng · S. Shanshan · X. Fei (✉) · W. Zhong
Jiangsu Key laboratory of Crop Genetics and Physiology/
Co-Innovation Center for Modern Production Technology of Grain Crops, Yangzhou University, Yangzhou 225009, China
e-mail: feixiong@yzu.edu.cn

Abbreviations

ATCs	Aleurone transfer cells
DAA	Days after anthesis
ECCs	Endosperm conducting cells
NPTCs	Nucellar projection transfer cells
NTTs	Nutrient transfer tissues
SETCs	Starchy endosperm transfer cells

Introduction

Wheat (*Triticum aestivum* L.) is one of the most commercially important food crops, accounting for more than 30 % of global food production. The amount of starch and protein accumulated in wheat grain are considered major determinants of wheat yield and quality (Bechtel et al. 2009; Shewry et al. 2009, 2012). Since these nutrients are commonly delivered to endosperm via caryopsis nutrient transfer tissues (NTTs), elucidation of NTTs development is paramount to developing an understanding of control of assimilate partitioning (Domínguez et al. 2001; Xiong et al. 2013b; Zhou et al. 2009).

The process and pathway of nutrient transport have received extensive study (Cochrane 1983; Sakri and Shannon 1975; Wang and Fisher 1994; Wang et al. 1994a, 1995a, b; Patrick and Offler 2001). During grain filling, nutrients are first imported to the caryopsis through the spikelet phloem and then via the vascular bundle within the caryopsis pericarp (Ugalde and Jenner 1990a, b). There are no symplastic connections between the maternal tissues and the endosperm (Zheng and Wang 2011), and nutrients from maternal tissues are released into a specialized apoplastic cavity derived from schizogenous activity (Patrick and Offler 2001).

Subsequently, nutrients are taken up from the apoplastic cavity and move radially throughout the starchy endosperm via filial compartments (Ugalde and Jenner 1990a). Not surprisingly, therefore, the transport processes within the maternal tissues of the wheat grain play a vital and dynamic role in determining the rate of assimilate import into the grain (Wang and Fisher 1994).

The tissues involved in transfer from the crease region of the caryopsis include maternal transfer tissues and endosperm transfer tissues. In particular, the

absence of symplastic linkage between maternal and filial generations permits independent investigation of nutrient transport and metabolism in these two tissues (Patrick and Offler 2001). The maternal transfer tissues are sequentially composed of vascular bundle, chalaza, and nucellar projection transfer cells (NPTCs), while endosperm transfer tissues sequentially consist of aleurone transfer cells (ATCs, also called "modified aleurone cells"), starchy endosperm transfer cells (SETCs, also called "sub-aleurone cells"), and endosperm conducting cells (ECCs). The structure and developmental anatomy
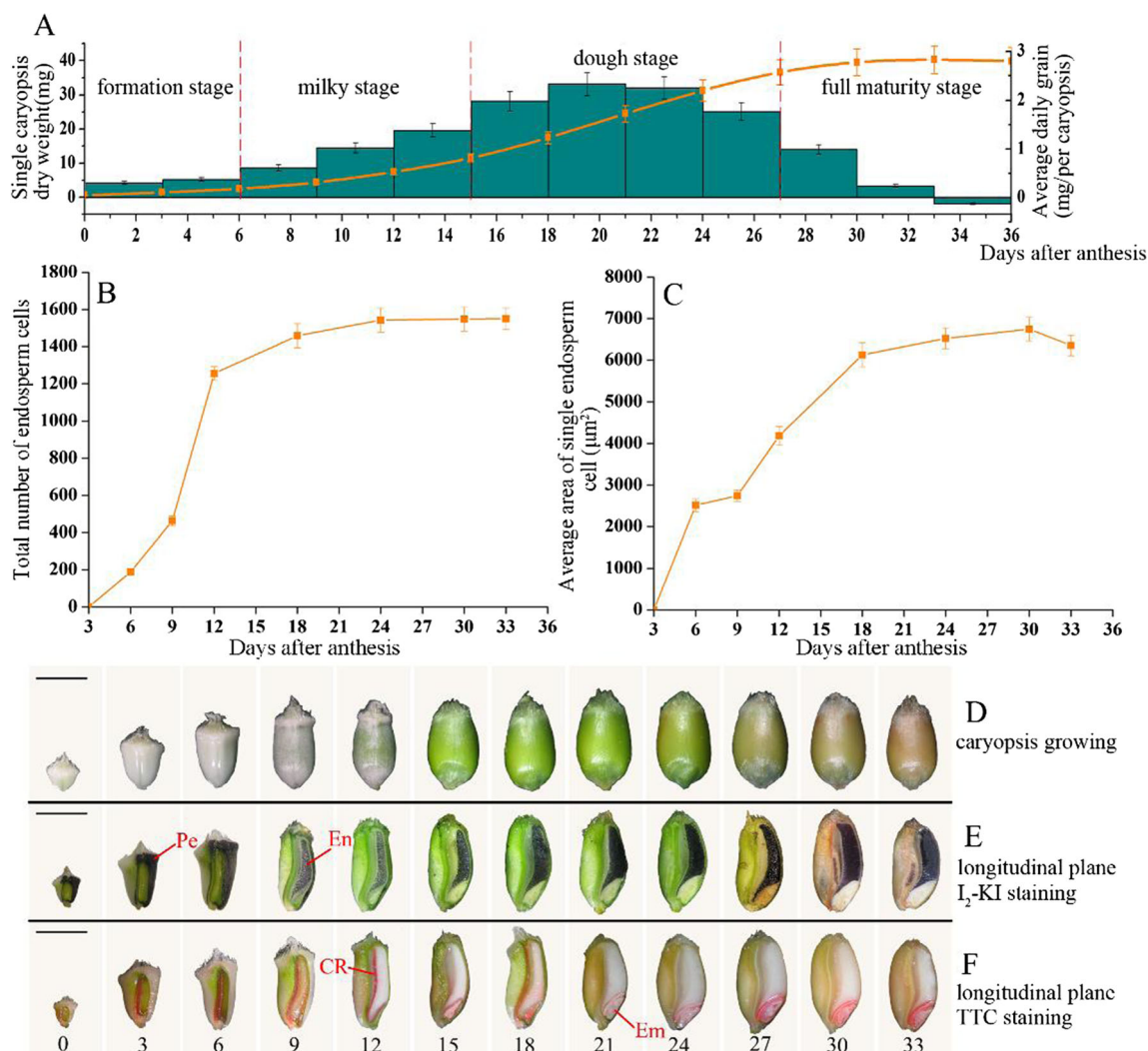

Fig. 1 Caryopsis growth. *Line plot* shows temporal changes in dry weight of caryopsis and *bar chart* shows the average daily gain per caryopsis at different days after anthesis (DAA) (**a**). Five caryopses were combined into one sample. Data points are the means of three replicate caryopses (15 caryopses total) with the standard error of each shown as a *vertical bar*. Total number of endosperm cells in transverse section of caryopsis center (**b**) and average area of single endosperm cell in transverse section of caryopsis center (**c**). Data points were the means of three

replicate caryopses with the standard error of each shown as a *vertical bar*. Caryopsis profile (**d**). Longitudinal section of caryopsis stained by I₂/KI (**e**) and by 2,3,5-triphenyl-2H-tetrazolium chloride (**f**). *Numbers* below **d**–**f** indicate the DAA. The *red parts* show the positions where the activity of dehydrogenase is high and the *black parts* are the positions where starch is accumulated. *CR* crease region, *Em* embryo, *En* endosperm, *Pe* pericarp. *Scale bars* 4 mm (**d**–**f**)

of some NTTs have received extensive study. Felker et al. (1984) sectioned the crease region of the developing barley caryopsis and presented micrographs that showed ultrastructure of the vascular bundle and chalaza. Wang et al. (1994b) and Thompson et al. (2001) detailedly studied the development of NPTCs; furthermore, Zheng and Wang (2011) compared the SETCs and NPTCs; however, little information is available concerning ATCs, SETCs, and ECCs. Moreover, the literature above indicates no integrated investigation of the structural development of the entire NTTs and their functions, particularly those involved in the relationship between development of NTTs and endosperm growth. An investigation of the structural development and probable function of the NTTs in wheat caryopsis was made in the present study. Additionally, the pathway of nutrient transfer from the vascular bundle to starchy endosperm and the embryo was also discussed. The findings not only provided an anatomic basis for interpreting the relationship between structure and function of NTTs but also were used to further clarify their relationships with endosperm and embryo development.

Material and methods

Plant materials

Wheat (*T. aestivum* L.) cv. Yangmai13, a soft winter wheat, is widely grown in China and was provided by the National Wheat Improvement Center. The experiment was conducted in the research field of Yangzhou University, Jiangsu, China from 1 November 2012 (sowing) to 10 June 2013. Individual florets were marked with a pen and tagged to determine the anthesis date. Developing caryopses were harvested at the different dates for further study.

Dry weight determination of developing caryopses

Wheat caryopses were collected every 3 days after anthesis (DAA) and dried in a fan-forced oven at 105 °C for 1 h to deactivate enzymes and then at 80 °C for 72 h to attain constant weights for dry weight determination. Average daily gain was calculated according to the dry weights of caryopses.

Sample observation under stereoscopic microscope

Caryopses at different DAA were cut longitudinally from the center by hand and stained with I_2/KI solution (0.3 % iodine and 1 % potassium iodide) for 1 min and then with 0.5 % 2,3,5-triphenyl-2H-tetrazolium chloride for 30 min. All sections and their corresponding caryopses were photographed under stereoscopic microscope (MZ6, Leica, Germany) equipped with a digital camera (Powershot S70, Canon, Japan).

Sample observation under light microscope

Caryopses at different DAA were harvested and cut longitudinally or transversely into 2-mm thick slice from the middle

Fig. 2 Light microscope images of transverse sections of caryopsis (**a**), vascular parenchyma and chalaza (**b**, higher magnification view of *1 black box* in **a**), nucellar projection (**c**, higher magnification view of *2 black box* in **a**), and endosperm free nucleus (**d**, higher magnification view of *3 black box* in **a**) in wheat caryopsis at 3 DAA. *CH* chalaza, *CR* crease region, *FN* free nucleus, *NC* nucellar cell, *NP* nucellar projection, *Nu* nucleus, *Pe* pericarp, *V* vacuole, *VP* vascular parenchyma. *Scale bars* 400 μm (**a**) and 20 μm (**b–d**)
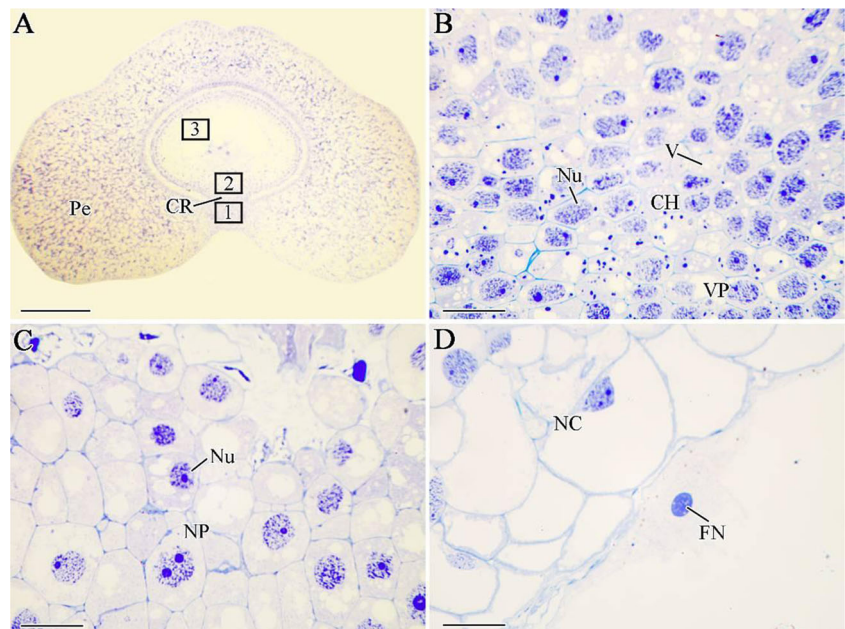
of the caryopses with a razor blade and immediately fixed in a fixative containing 2.5 % glutaraldehyde and 1 % paraformaldehyde in 50 mM Na cacodylate buffer (pH 7.2) at 4 °C for 3 h. Tissue slices were dehydrated in a graded ethanol series followed by propylene oxide and embedded in SPI low-viscosity Spurr's resin (Spurr 1969). Sections of 1-µm thickness were cut using a Ultracut rotary microtome (Ultracut R, Leica, Germany) and stained with 0.5 % toluidine blue O in 2.5 % sodium carbonate for 10 min, rinsed, dried, and examined by light microscope (DMLS, Leica, Germany). Photographs were taken with a digital camera (D5000, Nikon, Thailand).

### Sample observation under scanning electron microscope

Fresh caryopses were selected at 18 DAA and immediately frozen in liquid nitrogen for 30 s, after which the grains were cut transversely and soaked in a fixative containing 2.5 % glutaraldehyde and 1 % paraformaldehyde in 50 mM Na cacodylate buffer (pH 7.2) at 4 °C for 3 h. Then, samples were rinsed thrice with 0.1 M phosphate buffer (pH 7.2) and dehydrated in an ethanol series of 20, 40, 60, 80, 90, 95, and 100 %. Afterward, ethanol was replaced by isoamyl acetate. Samples were dried in a critical point dryer, sputter-coated with gold, and viewed under a scanning electron microscope (XL-30, Philips, Holland) at 20 kV.

Determination of cell number and cell size

Microscope images were obtained from the digital camera. The total number of endosperm cells and average area of single endosperm cell were calculated using Image-Pro Plus software (Version 6.0, Media Cybernetics, USA).

Fig. 3 Light microscope images of transverse sections of caryopsis (**a**), sieve tubes (**b**), chalaza (**c**), nucellar projection (**d**), endosperm cells opposite apoplastic cavity (**e**), starchy endosperm cells (**f**), and nucellus (**g**) in wheat caryopsis at 6 DAA. *AC* apoplastic cavity, *CH* chalaza, *En* endosperm, *lNP* lower nucellar projection, *mNP* middle nucellar projection, *NP* nucellar projection, *Nu* nucleus, *Pe* pericarp, *SG* starch granule, *ST* sieve tube, *TW* thickened wall, *uNP* upper nucellar projection, *V* vacuole, *VB* vascular bundle, *VP* vascular parenchyma. *Scale bars* 300 µm (**a**) and 20 µm (**b**–**g**)
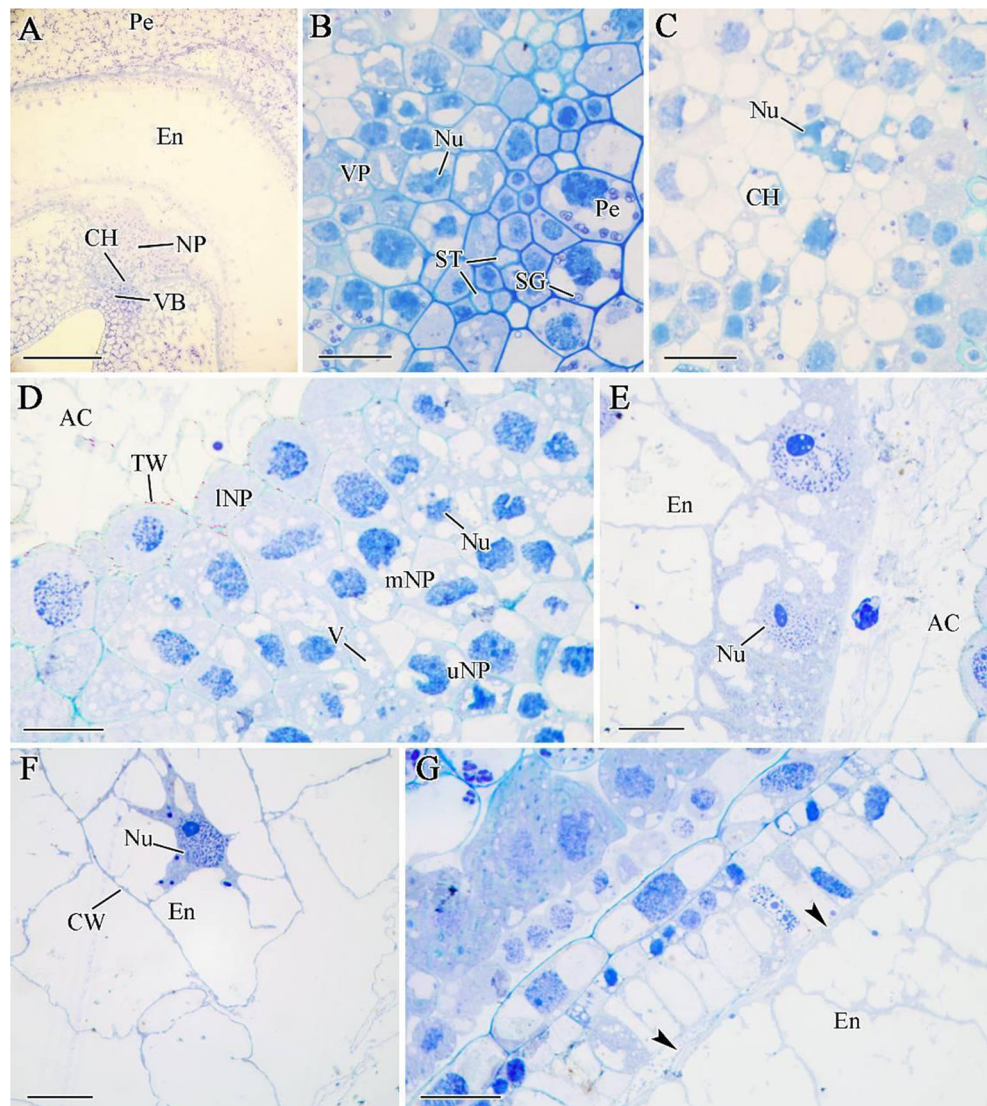
Statistical analysis

Statistical analyses of the data were conducted using SPSS Statistics (Version 19.0, International Business Machines Corporation, USA). All the figures were produced using Adobe Photoshop software (Version CS4, Adobe, USA).

Results

Overall developmental process of the wheat caryopsis

The dry weight of caryopses increases slowly during 0–6 DAA, then increased quickly during 9–27 DAA with average daily gain of 1.8 mg/day, reached its maximum value at 30 DAA and decreased slowly thereafter (Fig. 1a).

The total number of endosperm cells and average area of single endosperm cell at the center of transverse section micrographs were calculated using software, and the results are shown in Fig. 1b, c. Obviously, the total number of endosperm cells initially increased rapidly from 3 to 12 DAA and subsequently increased slowly (Fig. 1b). Average area of single endosperm cell increased rapidly from 3 to 6 DAA and 9 to 18 DAA and decreased after 30 DAA (Fig. 1c). This indicated that the rapid cell division (3–12 DAA) and cell elongation (3–18 DAA) were in preparation for an increased accumulation of storage products.

During 0–9 DAA, the ovary continually expanded but developed much faster in the longitudinal axis and attained its full length in the kernel at 9 DAA (Fig. 1d). The caryopsis appeared white. During 9–21 DAA, the caryopsis increased in volume and became green. During 21–30 DAA, the caryopsis volume changed little and slowly turned yellow. During

Fig. 4 Light microscope images of transverse sections of caryopsis (**a**), sieve tubes (**b**), chalaza (**c**), nucellar projection (**d**), aleurone transfer cell (**e**), central starchy endosperm (**f**), and aleurone layer (**g**) in wheat caryopsis at 9 DAA. *AL* aleurone layer, *ATC* aleurone transfer cell, *CH* chalaza, *CSE* central starchy endosperm, *En* endosperm, *lNP* lower nucellar projection, *mNP* middle nucellar projection, *NP* nucellar projection, *Nu* nucleus, *Pe* pericarp, *SG* starch granule, *ST* sieve tube, *TW* thickened wall, *uNP* upper nucellar projection, *V* vacuole, *VB* vascular bundle, *VP* vascular parenchyma. *Scale bars* 500 μm (**a**) and 20 μm (**b**–**g**)
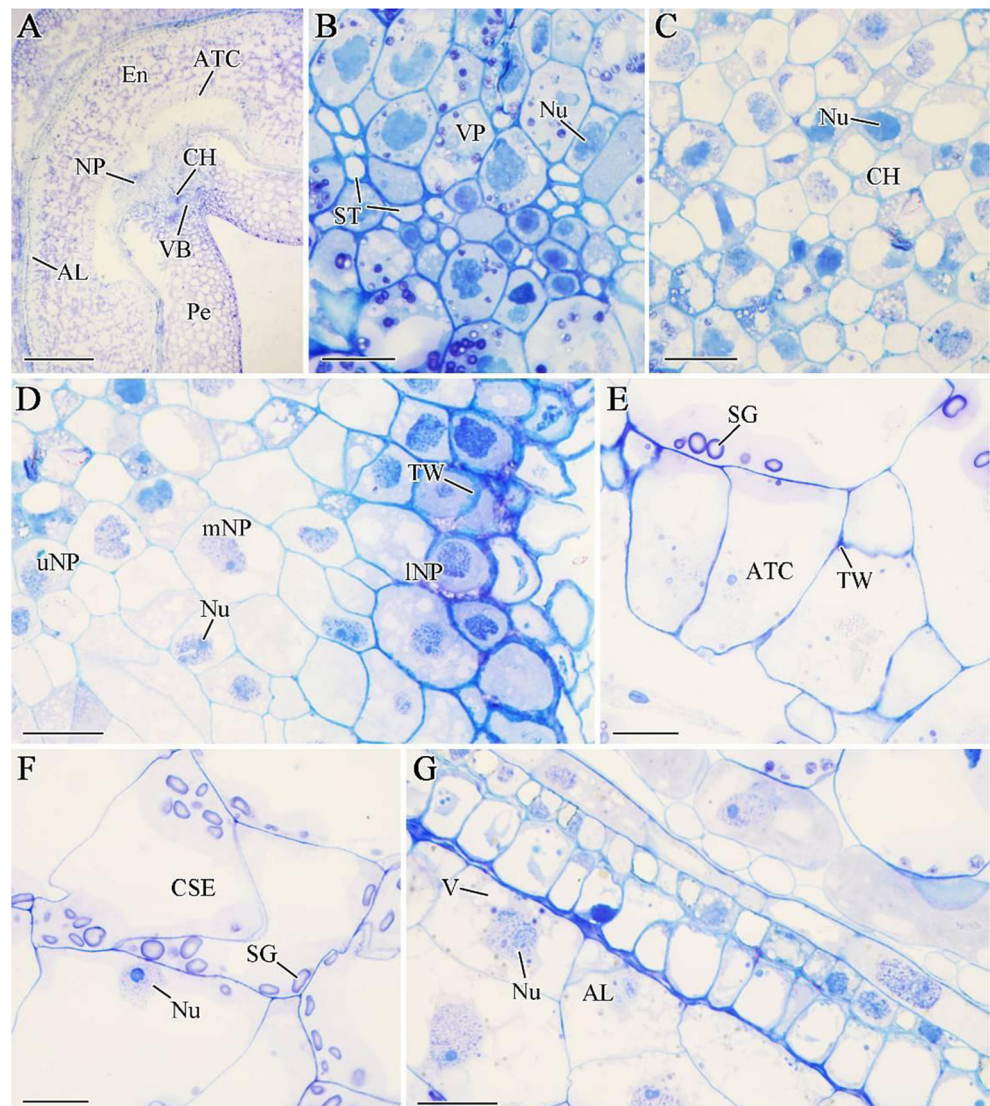
maturity (after 30 DAA), the caryopsis became yellow and hard (Fig. 1d).

From anthesis to maturation, the endosperm was stained increasingly with I$_2$/KI (Fig. 1e), showing that starch mainly accumulated in the endosperm, while pericarp was stained decreasingly with I$_2$/KI, indicating gradual disappearance of the starch accumulated in pericarp (Xiong et al. 2013a). During 0–12 DAA, the crease region including vascular bundle, chalaza, and nucellar projection were increasingly stained with 2,3,5-triphenyl-2H-tetrazolium chloride, indicating that dehydrogenase activity increased after anthesis and attained a maximum at 12 DAA (Fig. 1f). During 12–21 DAA, the color faded away; at the same time, the embryo had formed and was most deeply stained, showing that it had high activity and vigorous respiration (Fig. 1f). The starchy endosperm was not stained, showing that its cells were dead (Wang et al. 2012).

The structural changes of NTTs in developing caryopses

Caryopsis sections fixed in the same conditions were used for light microscopy, stereoscopic microscopy, and scanning electron microscopy to take advantage of various observation scales. Developmental stages analyzed in this study covered 3–33 DAA (Figs. 2, 3, 4, 5, 6, 7, 8, 9, and 10). Based on the structural and functional characteristics of NTTs in developing caryopses, we divided the developmental process into four stages: initiation (before 3 DAA), differentiation (3–12 DAA), function (12–24 DAA), and apoptosis (after 24 DAA) stages.

Initiation stage

At 3 DAA, there were a number of parenchymal cells of uniform structure in the crease region of the caryopsis. Vascular bundle did not differentiate and sieve tubes were

Fig. 5 Light microscope images of longitudinal sections of caryopsis (**a**), higher magnification view of *1 black box* in **a** (**b**), higher magnification view of *2 black box* in **a** (**c**), and transverse sections of sieve tubes (**d**), chalaza (**e**), nucellar projection (**f**), aleurone transfer cells and starchy endosperm transfer cells (**g**), central starchy endosperm cells (**h**), and aleurone layer (**i**) in wheat caryopsis at 12 DAA. *AG* aleurone grain, *AL* aleurone layer, *ATC* aleurone transfer cell, *CH* chalaza, *CSE* central starchy endosperm, *ECC* endosperm conducting cell, *Em* embryo, *lNP* lower nucellar projection, *mNP* middle nucellar projection, *Nu* nucleus, *PB* protein body, *S* spherosome, *SETC* starchy endosperm transfer cell, *SG* starch granule, *ST* sieve tube, *TSE* tissues surrounding embryo, *TW* thickened wall, *TV* tannin vacuole, *uNP* upper nucellar projection, *V* vacuole, *VP* vascular parenchyma. *Scale bars* 300 μm (**a**), 50 μm (**b**), 100 μm (**c**), and 20 μm (**d**–**i**)
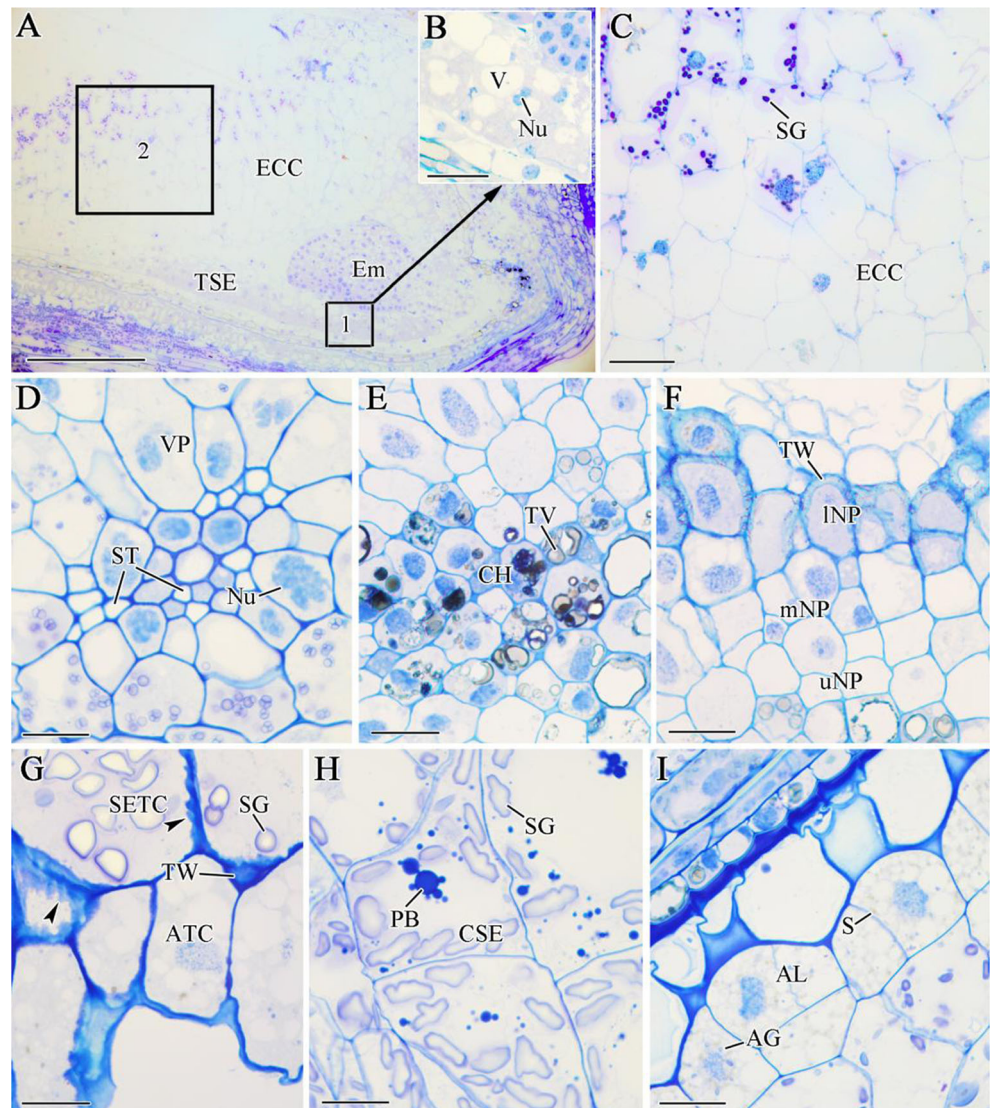
Fig. 6 Stereoscopic microscope image of longitudinal sections of caryopsis (**a**) and light microscope images of *white box* in **a** (**b**), higher magnification view of *1 black box* in **b** (**c**) and higher magnification view of *2 black box* in **b** (**d**) in wheat caryopsis at 18 DAA. *CSE* central starchy endosperm, *ECC* endosperm conducting cell, *Em* embryo, *Sm* scutum. Caryopsis at **a** was stained by I$_2$/KI. *Scale bars* 1 mm (**a**), 200 μm (**b**), 20 μm (**c**), and 50 μm (**d**)
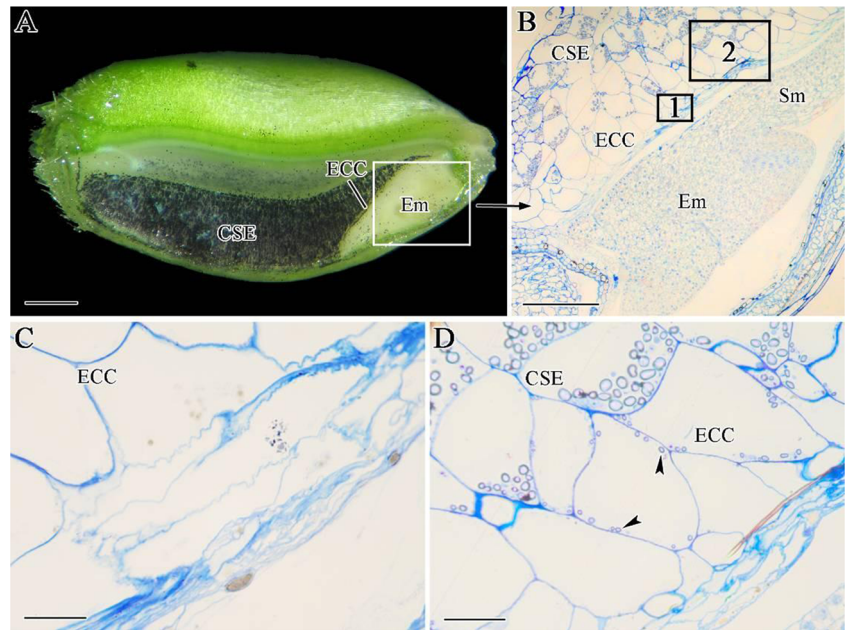
not observed (Fig. 2a, b), and the only obvious nucleus was in parenchymal cells. Chalaza cells, like parenchymal cells, also contained a large nucleus and many small vacuoles (Fig. 2b). Nucellar projection cells were large and contained a large

Fig. 7 Stereoscopic microscope image of transverse section of caryopsis (**a**) and light microscope images of transverse sections of sieve tubes (**b**), chalaza (**c**), nucellar projection cells (**d**), aleurone transfer cells and endosperm transfer cells (**e**), starchy endosperm cells (**f**), and aleurone layer (**g**) in wheat caryopsis at 18 DAA. *AG* aleurone grain, *AL* aleurone layer, *ATC* aleurone transfer cell, *CH* chalaza, *CR* crease region, *CSE* central starchy endosperm, *En* endosperm, *lNP* lower nucellar projection, *mNP* middle nucellar projection, *PB* protein body, *Sp* spherosome, *SETC* starchy endosperm transfer cell, *SG* starch granule, *ST* sieve tube, *TW* thickened wall, *TV* tannin vacuole, *uNP* upper nucellar projection, *VP* vascular parenchyma. *Arrowheads* in **e** indicate the wall ingrowths. *Scale bars* 2 mm (**a**) and 20 μm (**b**–**g**)
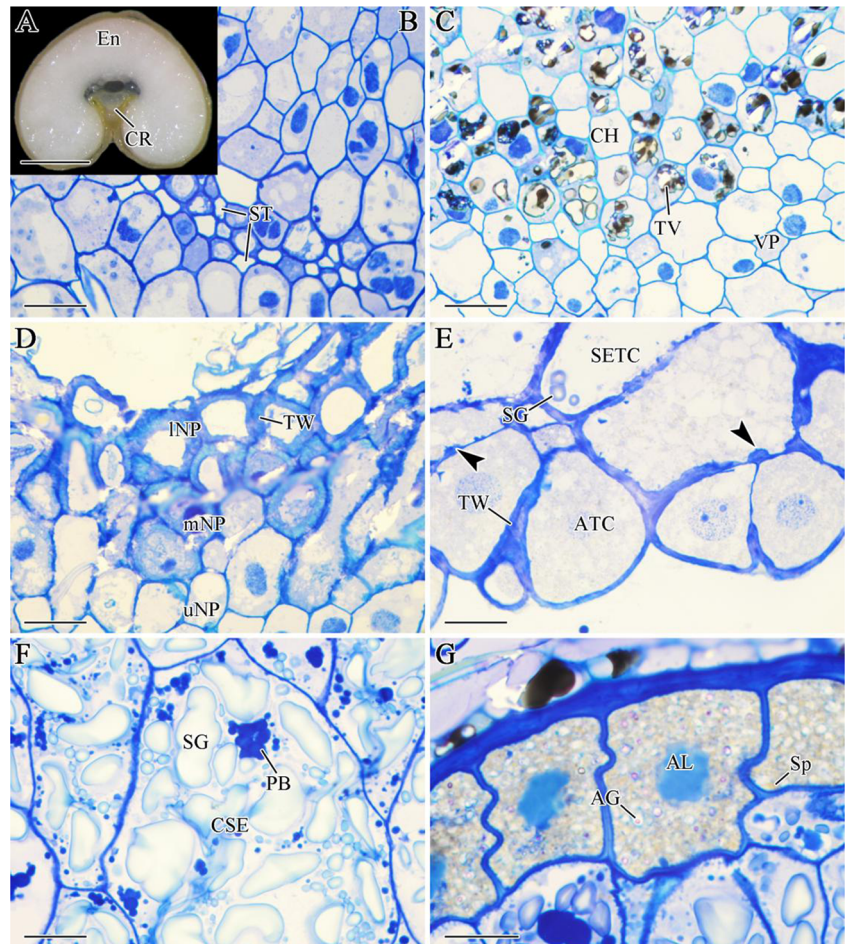
Fig. 8 Scanning electron microscope images of transverse section of caryopsis (**a**), sieve tubes and chalaza (**b**), nucellar projection transfer cells (**c**), higher magnification view of *white box* in **c** (**d**), aleurone transfer cells and endosperm transfer cells (**e**), starchy endosperm (**f**), and aleurone layer (**g**) in wheat caryopsis at 18 DAA. *AL* aleurone layer, *ATC* aleurone transfer cells, *CH* chalaza, *CR* crease region, *CSE* central starchy endosperm, *En* endosperm, *NPTC* nucellar projection transfer cell, *SETC* starchy endosperm transfer cell, *SG* starch granule, *ST* sieve tube, *TW* thickened wall, *WI* wall ingrowths. *Black arrowhead* in **a** shows inclusions in chalaza cells
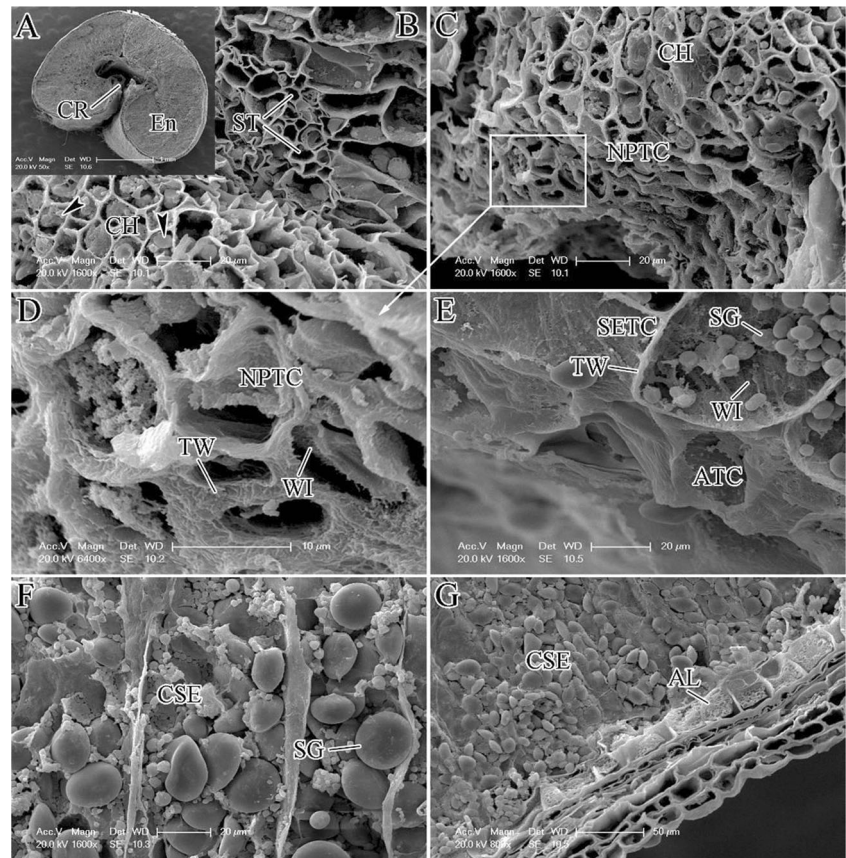
nucleus (Fig. 2c). At this time, endosperm was undergoing free nuclear stage and nucleus was clearly observed inside the nucellar cells (Fig. 2d).

Differentiation stage

At 6 DAA, the vascular bundle was mostly formed and a few sieve tubes were symplastically interconnected with the surrounding ground tissues, but vascular parenchymal cell nucleus had decreased in number (Fig. 3a, b). A larger number of chalaza cell nucleus had disappeared and cytoplasm obviously became light (Fig. 3c). It is probably that the disappeared nucleus and light cytoplasm reduced the cell-to-cell nutrient transport hindrance. The nucellar projection successively differentiated into upper, middle, and lower nucellar projections with specific structural and functional features (Fig. 3d). Upper nucellar projection cells contained an obvious nucleus and large vacuoles. Middle nucellar projection cells contained a large nucleus but small vacuoles. Lower nucellar projection cells contained few vacuoles and the outmost cell wall became thicker, indicating they were differentiating into NPTCs (Fig. 3d). The endosperm cells opposite the apoplastic cavity contained an obvious nucleus and denser cytoplasm (Fig. 3e). Central starchy endosperm cells were at cellularization stage and cell walls had formed (Fig. 3f). The nucellus degenerated

by a process of programmed cell death (arrowhead in Fig. 3g), as described by Domínguez et al. (2001).

At 9 DAA, the caryopsis further developed (Fig. 4a) and in the crease region, sieve tubes progressively increased in number but the vascular parenchymal cell nucleus had further decreased in number (Fig. 4b). The nucleus and cytoplasm of chalaza cells disappeared further (Fig. 4c). The nucellar projection differentiated further, with upper nucellar projection cells becoming smaller, while middle nucellar projection cells became larger and lower nucellar projection cells fully differentiated into NPTCs with thickened walls (Fig. 4d). At this stage, NPTCs have been definitively identified as the maternal cells responsible for nutrient release (Wang et al. 1994b). The endosperm cells opposite apoplastic cavity began to differentiate into ATCs with thicker walls, and adjoining cells separated near the apoplastic cavity (Fig. 4e). Central starchy endosperm cell nucleus began to die, and they differentiated into central endosperm storage cells containing some starch granules (Fig. 4f). The cells in the outermost one to two layers of endosperm began to differentiate into the aleurone layer (Fig. 4g) (Xiong et al. 2013b).

At 12 DAA, the young embryo was surrounded by ECCs and tissues surrounding embryo (Fig. 5a) which

Fig. 9 Light microscope images of longitudinal sections of embryo, scutum, and central starchy endosperm (**a**), higher magnification view of *black box* in **a** (**b**) and transverse sections of vascular bundles (**c**), chalaza (**d**), nucellar projection cells (**e**), aleurone transfer cells and starchy endosperm transfer cells (**f**), central starchy endosperm cells (**g**), and aleurone layer (**h**) in wheat caryopsis at 24 DAA. *AG* aleurone grain, *AL* aleurone layer, *ATC* aleurone transfer cell, *Ca* callose, *CCW* compressed cell wall, *CH* chalaza, *CSE* central starchy endosperm, *Em* embryo, *NPTC*, nucellar projection transfer cell, *PB* protein body, *SETC* starchy endosperm transfer cell, *SG* starch granule, *Se* scutellar epithelium, *Sm* scutum, *ST* sieve tube, *TW* thickened wall, *TV* tannic vacuole, *VP* vascular parenchyma. *Arrowheads* in **b** indicate the destructional endosperm cells and in **e** and **f**, the wall ingrowths. *Scale bars* 300 μm (**a**) and 20 μm (**b–h**)
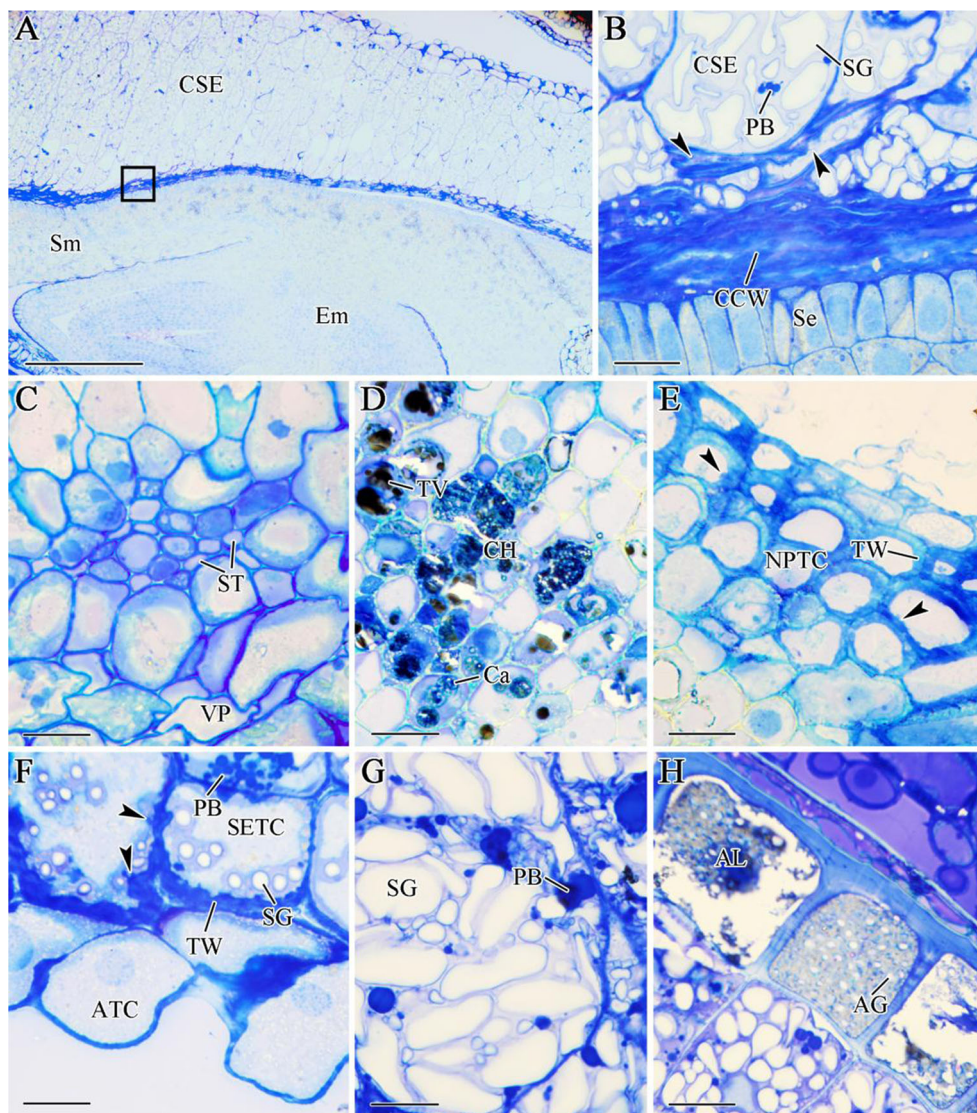
contain larger vacuoles, denser cytoplasm, and an obvious nucleus (Fig. 5b). The ECCs near the embryo contained no starch granules, while ECCs relatively far from the embryo contained a few starch granules (Fig. 5c). The vascular bundle matured and contained a number of sieve tubes; however, the parenchymal cell nucleus was markedly distorted and gradually disappeared (Fig. 5d). Tannic acid was observed in chalaza cell vacuoles (Fig. 5e), as also described in barley (Cochrane et al. 2000). The lower nucellar projection cell wall thickened further (Fig. 5f). The ATCs wall became thicker, forming wall ingrowths (Fig. 5g). The second and third layers of endosperm cells adjoining ATCs differentiated into SETCs with thicker walls and a few starch granules (Fig. 5g). Many starch granules and protein bodies were observed in central starchy endosperm cells (Fig. 5h). Of endosperm, one to two surface layers differentiated into aleurone layer cells

containing obvious nucleus, larger vacuoles, a few spherosomes, and aleurone grains (Fig. 5i).

Function stage

At 18 DAA, the ECCs near the scutum gradually became irregular, shrunken, and degenerated, finally forming a space between the scutum and ECCs (Fig. 6a–c), probably because the inclusions of these cells are absorbed by the scutum (Cosségal et al. 2007). The ECCs far from the scutum contained a few small starch granules (Fig. 6d), gradually differentiating into endosperm starch storage cells with many starch granules.

At 18 DAA, the number of sieve tubes increased further (Figs. 7b and 8b). The parenchymal cells near chalaza became irregular and apoptotic, and the vacuole in chalaza cells accumulated many tannic acid inclusions (Figs. 7c and 8b). Most

Fig. 10 Light microscope images of transverse sections of caryopsis (**a**), sieve tubes (**b**), chalaza (**c**), nucellar projection transfer cells (**d**), aleurone transfer cells and starchy endosperm transfer cells (**e**), central starchy endosperm cells (**f**), and aleurone layer (**g**) in wheat caryopsis at 33 DAA. *AG* aleurone grain, *AL* aleurone layer, *ATC* aleurone transfer cell, *CH* chalaza, *CSE* central starchy endosperm, *En* endosperm, *NPTC* nucellus projection transfer cell, *PB*, protein body, *SG* starch granule, *SETC* starchy endosperm transfer cell, *ST* sieve tube, *TW* thickened wall, *VB* vascular bundle, *VP* vascular parenchyma. *Scale bars* 500 μm (**a**) and 20 μm (**b–g**)
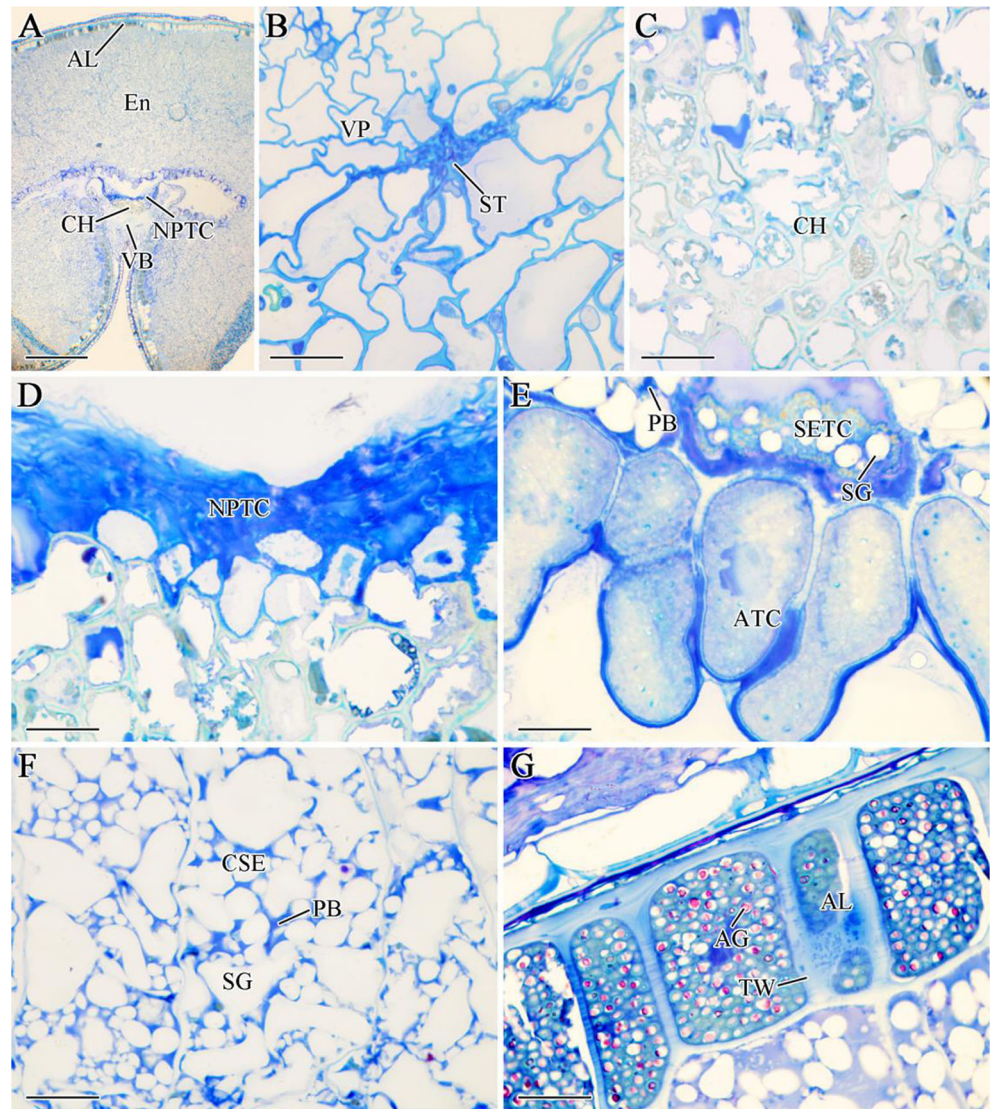
nucellar projection cells differentiated into NPTCs with thicker walls (Figs. 7d and 8c, d). At this stage, the ATCs and SETCs contained wall ingrowths (Figs. 7e and 8e). A large amount of starch granules and protein bodies had accumulated in the central starchy endosperm cells (Figs. 7f and 8f). The aleurone layer cells matured and contained many aleurone grains and spherosomes (Figs. 7g and 8g).
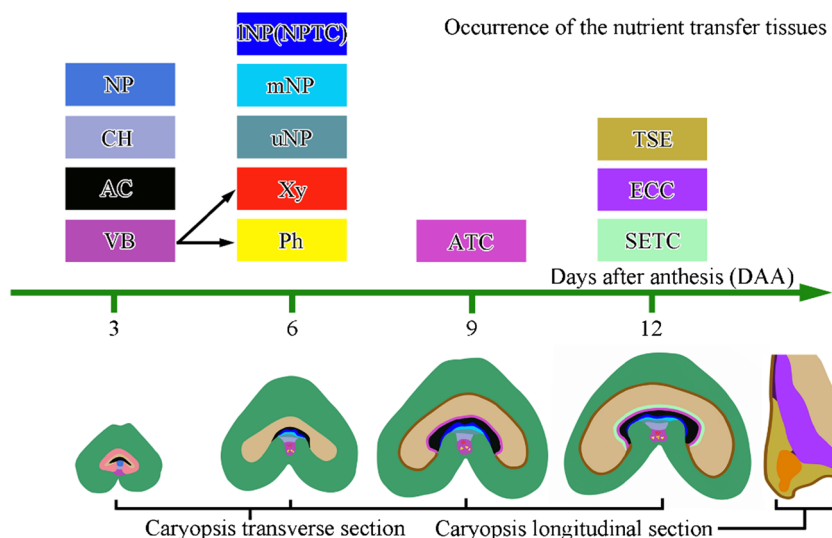
Apoptosis stage

At 24 DAA, the embryo was obviously enlarged and was well differentiated (Fig. 9a), as described by Smart and Obrien (1983). The epithelial cells of the scutum appeared thin and long (Fig. 9b). The reserves of ECCs near the scutum were absorbed by the scutum remaining compressed cell walls and there was extensive destruction of endosperm cells ahead of the scutum apex (Fig. 9b), while the ECCs far from the scutum

had almost differentiated into central endosperm storage cells with many starch granules and a few protein bodies (Fig. 9b). The vascular bundle began apoptosis, and notably, the parenchymal cells were distorted and their nucleus disappeared (Fig. 9c). Chalaza cells accumulated many inclusions including tannic acid and callose (Fig. 9d). Nucellar projection cells completely differentiated into NPTCs with much thicker walls and wall ingrowths (Fig. 9e). ATCs contained denser cytoplasm and thicker walls. SETCs contained many starch granules and protein bodies and their wall ingrowths were clearly observed (Fig. 9f). Central starchy endosperm was filled with starch granules and protein bodies (Fig. 9g). A large number of aleurone grains had accumulated in aleurone layer cells with thicker walls (Fig. 9h).

At 33 DAA, sieve tubes, especially parenchymal cells, were distorted and the depleted vascular bundle had begun to collapse (Fig. 10b). There was extensive destruction of

chalaza and nucellar projection cells (Fig. 10c, d). Chalaza cells shrank, their nucleus and cytoplasm disappeared, and they became empty cell lumina with only walls (Fig. 10c). NPTCs were wrinkled and fused, and residual bodies of these cells were clearly observed (Fig. 10d). ATCs contained denser cytoplasm and SETCs accumulated a few starch granules (Fig. 10e). Many starch granules and protein bodies filled the central starchy endosperm cells; furthermore, protein bodies were fused in starch granules (Fig. 10f). At this stage, the aleurone layer cells were fully mature, with thicker walls and a larger number of aleurone grains than previously (Fig. 10g).

Discussion

Although much literature have documented the structure of NTTs at the structural level, there have been no attempts to study the whole developmental process of all these tissues from anthesis to maturity and how their developments are integrated with endosperm and embryo. The initiation and subsequent development of these tissues showed patterns of temporal and spatial gradients. The time stamp of occurrence of NTTs was shown in Fig. 11, which covered each of the critical phases (3, 6, 9, and 12 DAA) of NTTs development. Moreover, we speculate that the pathway of nutrient transfer from vascular bundle to the starchy endosperm, aleurone layer and embryo in the developing wheat grain is as schematically represented in Fig. 12. Nutrients from the vascular bundle are unloaded into the NPTCs via chalaza, and then are transported into the central starchy endosperm and aleurone layer via ATCs and SETCs. The nutrients are also transported into the embryo through ATCs, SETCs, ECCs, and tissues surrounding embryo.

In previous studies, the endosperm and embryo growth had a strong relationship with the differentiation and development of NTTs of barley (Radchuk et al. 2011) and *Sorghum bicolor* (Wang et al. 2012). According to Bechtel et al. (2009), the phase of endosperm development can be defined in five phases: (1) formation of endosperm free nucleus, (2) cellularization of the layer of endosperm cells, (3) completion of meristematic activity, (4) attainment of maximum dry weight, and (5) harvest ripeness. Thereafter, along with the enrichment of starchy endosperm and desiccation of the caryopsis, the NTTs underwent programmed cell death and eventually lost their function of nutrient transfer; moreover, the degradation of NTTs is speculated to recover a portion of valuable resources (Wang et al. 2012).

Moreover, some genes were found to be involved in the development of NTTs. A gene *APL* is required for sieve tube
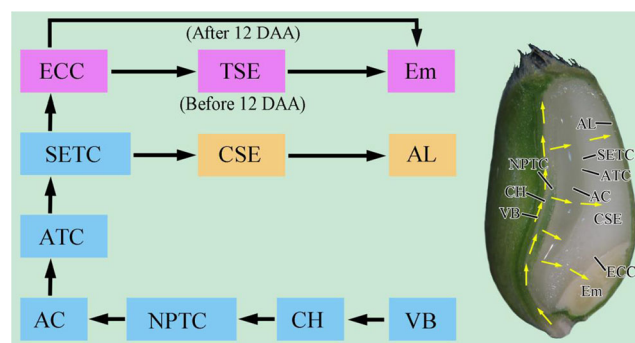

Fig. 12 Schematic representation of the pathway of nutrient transfer from vascular bundle to the aleurone layer and embryo in the developing wheat grain. *AC* apoplastic cavity, *AL* aleurone layer, *ATC* aleurone transfer cell, *CH* chalaza, *CSE* central starchy endosperm, *ECC* endosperm conducting cell, *Em* embryo, *NPTC* nucellar projection transfer cell, *SETC* starchy endosperm transfer cell, *TSE* tissues surrounding embryo, *VB* vascular bundle. *Black and yellow arrows* indicate the pathway of nutrient transport

differentiation but not sufficient for vascular differentiation (Carlsbecker and Helariutta 2005). The gene *JEKYLL* plays an important role in the nucellar projection differentiation (Radchuk et al. 2006), and gene *NUC1* is expressed in the nucellar projection after nucellus disappears (Doan et al. 1996). Thiel et al. (2008) have found that some cell wall biosynthesis and expansion/extension genes were related to nucellar projection differentiation. But it is still unknown whether these genes are related to the differentiation of NPTCs. A gene *ZmESR-6* is specifically expressed in tissues surrounding embryo, and its cDNA encodes a small protein homologous to plant defensins (Balandin et al. 2005). Gómez et al. (2002) reported that gene *ZmMRP-1* is a key regulator in the differentiation of SETCs. A protein encoded by *ZmMRP-1* was considered to transactivate promoters of endosperm transfer cell-specific gene *BETL-1* (Barrero et al. 2006), *MEG1* (Gutiérrez-Marcos et al. 2004), and *ZmTCRR-1* (Muñiz et al. 2006).

In comparison with other cereal crops, such as sorghum and maize, there are some obvious differences in the development of NTTs: (1) Small vascular region lies beside the apoplastic cavity in sorghum; large cup-like cushion consisted of many vascular terminals envelops the basal endosperm in maize; only one main vascular bundle is involved in the nutrient transport in wheat. (2) SETCs have few wall ingrowths and accumulate very few starch granules in sorghum; SETCs have long and dense wall ingrowths and do not accumulate starch granules in maize; SETCs have shorter and fewer ingrowths than sorghum and maize and accumulate more starch granules; (3) ECCs are elongated and accumulated very few starch granules in sorghum; ECCs in maize are elongated more obviously than in sorghum; ECCs are not elongated and do not accumulate starch granule in wheat (Zheng and Wang 2010; Zheng et al. 2014; Becraft and Gutierrez-Marcos 2012).

In conclusion, the NTTs of wheat caryopses initiated before 3 DAA (Fig. 2), differentiated during 3–12 DAA (Figs. 2, 3, 4, and 5), functioned during 12–24 DAA (Figs. 5, 6, 7, 8, and 9), and were apoptotic after 24 DAA (Figs. 9 and 10). The timing when NTTs was fully developed was consistent with the timing of average daily gain of caryopsis dry weight reaching a maximum. Therefore, the occurrence, development, and apoptosis of NTTs were closely related to caryopsis growth, especially the enrichment of endosperm and embryo growth.

Conflict of interest The authors have no conflicts of interest related to the material presented in this article.

References

Balandin M, Royo J, Gomez E, Muniz LM, Molina A, Hueros G (2005) A protective role for the embryo surrounding region of the maize endosperm, as evidenced by the characterization of *ZmESR-6*, a defensin gene specifically expressed in this region. Plant Mol Biol 58:269–282

Barrero C, Muñiz LM, Gómez E, Hueros G, Royo J (2006) Molecular dissection of the interaction between the transcriptional activator *ZmMRP-1* and the promoter of *BETL-1*. Plant Mol Biol 62:655–668

Bechtel DB, Abecassis J, Shewry PR, Evers AD (2009) Development, structure and mechanical properties of the wheat grain. In: Khan K, Shewry PR (eds) Wheat: chemistry and technology, 4th edn. AACC, St Paul, MN, USA, pp 51–95

Becraft PW, Gutierrez-Marcos J (2012) Endosperm development: dynamic processes and cellular innovations underlying sibling altruism. Wiley Interdiscip Rev Dev Biol 1:579–593

Carlsbecker A, Helariutta Y (2005) Phloem and xylem specification: pieces of the puzzle emerge. Curr Opin Plant Biol 8:512–517

Cochrane MP (1983) Morphology of the crease region in relation to assimilate uptake and water loss during caryopsis development in barley and wheat. Aust J Plant Physiol 10:473–491

Cochrane MP, Paterson L, Gould E (2000) Changes in chalazal cell walls and in the peroxidase enzymes of the crease region during grain development in barley. J Exp Bot 51:507–520

Cosségal M, Vernoud V, Depège N, Rogowsky PM (2007) The embryo surrounding region. In: Plant cell monographs. Olsen OA, ed. Berlin Heidelberg: Springer, monogr., 8:57–71

Doan DNP, Linnestad C, Olsen OA (1996) Isolation of molecular markers from the barley endosperm coenocyte and the surrounding nucellus cell layers. Plant Mol Biol 31:877–886

Domínguez F, Moreno J, Cejudo FJ (2001) The nucellus degenerates by a process of programmed cell death during the early stages of wheat grain development. Planta 213:352–360

Felker FC, Peterson DM, Nelson OE (1984) Development of tannin vacuoles in chalaza and seed coat of barley in relation to early chalazal necrosis in the *segl* mutant. Planta 161:540–549

Gómez E, Royo J, Guo Y, Thompson R, Hueros G (2002) Establishment of cereal endosperm expression domains: identification and properties of a maize transfer cell-specific transcription factor, *ZmMRP-1*. Plant Cell 14:599–610

Gutiérrez-Marcos JF, Costa LM, Biderre-Petit C, Khbaya B, O'Sullivan DM, Wormald M, Perez P, Dickinson HG (2004) Maternally expressed gene1 is a novel maize endosperm transfer cell-specific gene with a maternal parent-of-origin pattern of expression. Plant Cell 16:1288–1301

Muñiz LM, Royo J, Gómez E, Barrero C, Bergareche D, Hueros G (2006) The maize transfer cell-specific type-A response regulator *ZmTCRR-1* appears to be involved in intercellular signalling. Plant J 48:17–27

Patrick JW, Offler CE (2001) Compartmentation of transport and transfer events in developing seeds. J Exp Bot 52:551–564

Radchuk V, Borisjuk L, Radchuk R, Steinbiss HH, Rolletschek H, Broeders S, Wobusa U (2006) Jekyll encodes a novel protein involved in the sexual reproduction of barley. Plant Cell 18:1652–1666

Radchuk V, Weier D, Radchuk R, Weschke W, Weber H (2011) Development of maternal seed tissue in barley is mediated by regulated cell expansion and cell disintegration and coordinated with endosperm growth. J Exp Bot 62:1217–1227

Sakri FAK, Shannon JCS (1975) Movement of ^{14}C-labeled sugars into kernels of wheat (*Triticum aestivum* L.). Plant Physiol 55:881–889

Shewry PR, Underwood C, Wan Y, Lovegrove A, Bhandari D, Toole G, Mills ENC, Denyer K, Mitchell RAC (2009) Storage product

synthesis and accumulation in developing grains of wheat. J Cereal Sci 50:106–112

Shewry PR, Mitchell RAC, Tosi P, Wan Y, Underwood C, Lovegrove A, Freeman J, Toole GA, Mills ENC, Ward JL (2012) An integrated study of grain development of wheat (cv. Hereward). J Cereal Sci 56:21–30

Smart MG, Obrien TP (1983) The development of the wheat embryo in relation to the neighbouring tissues. Protoplasma 114:1–13

Spurr AR (1969) A low-viscosity epoxy resin embedding medium for electron microscopy. J Ultrastruct Res 26:31–43

Thiel J, Weier D, Sreenivasulu N, Strickert M, Weichert N, Melzer M, Czauderna T, Wobus U, Weber H, Weschke W (2008) Different hormonal regulation of cellular differentiation and function in nucellar projection and endosperm transfer cells: a microdissection-based transcriptome study of young barley grains. Plant Physiol 148: 1436–1452

Thompson RD, Hueros G, Becker H, Maitz M (2001) Development and functions of seed transfer cells. Plant Sci 160:775–783

Ugalde TD, Jenner CF (1990a) Substrate gradients and regional patterns of dry matter deposition within wheat endosperm. I. Carbohydrates. Aust J Plant Physiol 17:377–394

Ugalde TD, Jenner CF (1990b) Route of substrate movement into wheat endosperm. I. Carbohydrates. Aust J Plant Physiol 17:693–704

Wang N, Fisher DB (1994) Monitoring phloem unloading and post-phloem transport by microperfusion of attached wheat grains. Plant Physiol 104:7–16

Wang HL, Offler CE, Patrick JW, Ugalde TD (1994a) The cellular pathway of photosynthate transfer in the developing wheat grain. I. Delineation of a potential transfer pathway using fluorescent dyes. Plant Cell Environ 17:257–266

Wang HL, Offler CE, Patrick JW (1994b) Nucellar projection transfer cells in the developing wheat grain. Protoplasma 182:39–52

Wang HL, Offler CE, Patrick JW (1995a) The cellular pathway of photosynthate transfer in the developing wheat-grain. II. A structural analysis and histochemical studies of the pathway from the crease phloem to the endosperm cavity. Plant Cell Environ 18:373–388

Wang HL, Patrick JW, Offler CE, Wang XD (1995b) The cellular pathway of photosynthate transfer in the developing wheat-grain. III. A structural analysis and physiological-studies of the pathway from the endosperm cavity to the starchy endosperm. Plant Cell Environ 18:389–407

Wang HH, Wang Z, Wang F, Gu YJ, Liu Z (2012) Development of basal endosperm transfer cells in *Sorghum bicolor* (L.) Moench and its relationship with caryopsis growth. Protoplasma 249:309–321

Xiong F, Yu XR, Zhou L, Wang F, Xiong AS (2013a) Structural and physiological characterization during wheat pericarp development. Plant Cell Rep 32:1309–1320

Xiong F, Yu XR, Zhou L, Wang Z, Wang F, Xiong AS (2013b) Structural development of aleurone and its function in common wheat. Mol Biol Rep 40:6785–6792

Zheng YK, Wang Z (2010) Current opinions on endosperm transfer cells in maize. Plant Cell Rep 29:935–942

Zheng Y, Wang Z (2011) Contrast observation and investigation of wheat endosperm transfer cells and nucellar projection transfer cells. Plant Cell Rep 30:1281–1288

Zheng YK, Wang Z, Gu YJ (2014) Development and function of caryopsis transport tissues in maize, sorghum and wheat. Plant Cell Rep 33:1023–1031

Zhou Z, Wang L, Li J, Song X, Yang C (2009) Study on programmed cell death and dynamic changes of starch accumulation in pericarp cells of *Triticum aestivum* L. Protoplasma 236:49–58